The vibration-rotation emission spectrum of hot BeF$_2$

Shanshan Yu, Alireza Shayesteh, and Peter F. Bernath[a)]
Department of Chemistry, University of Waterloo, Waterloo, Ontario N2L 3G1, Canada

Jacek Koput
Department of Chemistry, Adam Mickiewicz University, Grunwaldzka 6, 60-780 Poznan, Poland

The high-resolution infrared emission spectrum of BeF$_2$ vapor at 1000 °C was rotationally analyzed with the assistance of large-scale *ab initio* calculations using the coupled-cluster method including single and double excitations and perturbative inclusion of triple excitations, in conjunction with correlation-consistent basis sets up to quintuple-zeta quality. The ν_3 fundamental band, the $\nu_1 + \nu_2$, $\nu_1 + \nu_3$, and $2\nu_2 + \nu_3$ combination bands, and 18 hot bands were assigned. The symmetric stretching (ν_1), bending (ν_2), and antisymmetric stretching (ν_3) mode frequencies were determined to be 769.0943(2), 342.6145(3), and 1555.0480(1) cm^{-1}, respectively, from the band origins of the ν_3, $\nu_1 + \nu_3$, and $\nu_1 + \nu_2$ bands. The observed vibrational term values and B rotational constants were fitted simultaneously to an effective Hamiltonian model with Fermi resonance taken into account, and deperturbed equilibrium vibrational and rotational constants were obtained for BeF$_2$. The equilibrium rotational constant (B_e) was determined to be 0.235 354(41) cm^{-1}, and the associated equilibrium bond distance (r_e) is 1.3730(1) Å. The results of our *ab initio* calculations are in remarkably good agreement with those of our experiment, and the calculated value was 1.374 Å for the equilibrium bond distance (r_e). As in the isoelectronic CO$_2$ molecule, the Fermi resonance in BeF$_2$ is very strong, and the interaction constant k_{122} was found to be 90.20(4) cm^{-1}. © *2005 American Institute of Physics*. [DOI: 10.1063/1.2039085]

I. INTRODUCTION

In 1991, our group published a paper on the high-resolution infrared emission spectrum of BeF$_2$.[1] A series of spectra were recorded at temperatures ranging from 500 to 1000 °C. The spectrum obtained at around 700 °C was the best one (with the least amount of congestion but good intensity) and was analyzed. The eight vibration-rotation bands in the ν_3 fundamental region near 1550 cm^{-1} were assigned, and the antisymmetric stretching frequency ν_3 was determined. The present paper reports on the analysis of the spectrum recorded with the BeF$_2$ vapor at 1000 °C, in which the combination bands are much stronger.

The geometry of triatomic metal halide molecules has been a topic of discussion in many papers. The extensive experimental and computational studies have been reviewed recently by Hargittai.[2] The experimental studies include electron diffraction, photoelectron spectroscopy, matrix isolation, Raman spectroscopy, infrared emission and absorption, and laser-induced fluorescence. The application of these experimental techniques to the determination of metal halide structure was reviewed recently by Beattie,[3] and the problems and limits were discussed in detail.[2,3] The electron-diffraction method was the most used, and the equilibrium structures determined by this method are tabulated in the review by Spiridonov *et al.*[4] There are extensive low-resolution spectroscopic studies, but very little high-resolution data with resolved rotational structure is available. High-resolution spectroscopy is one of the most reliable methods used to determine molecular geometries, and is available only for a few metal dihalides, e.g., BeF$_2$,[1] FeCl$_2$,[5] NiCl$_2$,[6,7] and CuCl$_2$.[8]

The major interest in metal dihalides concerns whether they are linear or bent. The early electron-diffraction studies by Akishin *et al.*[9,10] suggested linear geometries for all alkaline earth dihalides although the bending angles were determined with large errors ($\pm 30° - 40°$). Simple bonding rules such as the valence-shell electron-pair repulsion (VSEPR) theory and Walsh's rules predicted linear geometries for all alkaline earth dihalides and it was generally believed that these bonding rules were reliable. Klemperer and co-workers,[11–13] however, used the technique of molecular-beam deflection by an inhomogeneous electric field to show that CaF$_2$, SrCl$_2$, and SrF$_2$, and all of the barium dihalides have permanent dipoles and are therefore bent. These results were confirmed later by the observation of the infrared and Raman spectra of the alkaline earth dihalides in matrices.[1,2,14–21] It was noted that the alkaline earth halides become increasingly bent as the metal becomes heavier and the halogen becomes lighter.

The failure of the VSEPR model and Walsh's rules to predict these bent structures prompted the development of improved models. Two physical models, *d*-orbital participation[22–31] and core polarization,[11,12,32–45] were used to explain these unexpected bent structures and have been discussed in detail in the reviews by Hargittai[2] and Kaupp.[46] In the *d*-orbital participation model, the lighter metals (e.g., Be and Mg) have only valence *ns* and *np* orbitals for covalent

---

[a)]Electronic mail: bernath@uwaterloo.ca

bonding leading to *sp* hybridization, which results in a linear structure. The heavier metals (e.g., Ca, Sr, and Ba) may employ their low-lying $(n-1)d$ orbitals for *sd* hybridization, which results in a nonlinear structure. In the core-polarization model, ionic ligands induce an angle-dependent dipole moment on the large, polarizable central ion of a MX_2 molecule, which stabilizes the bent structure relative to the linear structure. These two models appear to be inconsistent at first sight and have been discussed over many years. It has been argued[2,46–50] that both core polarization and *d*-orbital participation play a role in bonding in these molecules, and they are not strictly separable and "are the two sides of the same coin." For example, *d*-orbitals participate strongly in the bonding as determined by *ab initio* calculations and are also required to compute reliable polarizabilities. Von Szentpaly and Schwerdtfeger[48] and von Szentpaly[50] proposed the use of a "softness criterion," which combined elements of these two models. Unfortunately, this criterion does not account for the structures of all the alkaline earth dihalides.[46,49] No simple model has been found yet to account for the bent versus linear structures.

It is now established that all beryllium and magnesium dihalides are linear, SrF_2 and the barium dihalides are bent, and the others are "quasilinear" with a small barrier to linearity.[2,28,46] The linear structure of BeF_2 was first confirmed by the failure to observe the refocusing of the molecular beam by an electric field.[12] Büchler and Klemperer[51] investigated the low-resolution gas-phase infrared spectrum of BeF_2 and they assigned bands at 825 and 1520 cm^{-1} to the ν_2 and ν_3 vibrational frequencies, with the ν_2 frequency turning out to be a misassignment. In the matrix isolation work of Snelson,[15] ν_2 and ν_3 were determined to be 345 and 1555 cm^{-1} with an empirical correction for the matrix shifts. Our previous study[1] was the first high-resolution study of BeF_2, and the ν_3 frequency and the equilibrium bond distance were determined to be 1555.047 92(5) cm^{-1} and 1.372 971 0(95) Å, respectively. Later, an equilibrium bond length of 1.374(4) Å was redetermined from a gas-phase electron-diffraction experiment.[52] In Hargittai's latest review,[2] the gas-phase ν_1, ν_2, and ν_3 frequencies are estimated to be 760 ± 14, 334, and 1544 cm^{-1}, respectively. The value of ν_1 was estimated to be 680 cm^{-1} by Snelson[15] from the valence force constants and 594 ± 60 cm^{-1} by Vogt *et al.*[52] based on the force constants estimated from electron-diffraction results. There are only a few calculations at correlated levels of theory[53–56] on the structure and vibrational frequencies of BeF_2. In the recent study by Lee and Wright,[56] the best theoretical value for the equilibrium BeF bond length was estimated to be 1.380 ± 0.005 Å, and the ω_1, ω_2, and ω_3 harmonic frequencies were predicted to be in the ranges of 715–733, 345–357, and 1555–1597 cm^{-1}, respectively.

In this work, the ν_3 fundamental band, the $\nu_1+\nu_2$, $\nu_1+\nu_3$, and $2\nu_2+\nu_3$ combination bands, and 18 hot bands were assigned with the assistance of large-scale *ab initio* calculations. The ν_1, ν_2, and ν_3 vibrational frequencies were directly obtained by fitting most of these bands together. The observed vibrational term values and B rotational constants were fitted simultaneously to obtain the traditional equilib-

TABLE I. Molecular parameters for the ground electronic state of BeF_2 determined using the CCSD(T) method and various cc-pVnZ basis sets.

Property	cc-pVTZ	cc-pVQZ	cc-pV5Z
r_e(BeF) (Å)	1.3821	1.3784	1.3786
Energy+214 (hartree)	−0.332 863	−0.403 767	−0.427 207
r_e(BeF) (Å)[a]	1.3837	1.3798	1.3791
Energy+214 (hartree)	−0.351 545	−0.410 704	−0.429 874

[a]With the aug-cc-pVnZ basis set for fluorine.

rium vibrational and rotational constants for BeF_2.

II. *AB INITIO* PREDICTION OF THE VIBRATION-ROTATION ENERGY LEVELS

The equilibrium structure and three-dimensional potential-energy surface of BeF_2 were calculated using the coupled-cluster method including single and double excitations and a perturbation correction due to connected triple excitations[57–60] [CCSD(T)] in conjunction with the correlation-consistent valence basis sets up to quintuple-zeta quality (cc-pV5Z).[61] In the valence correlation treatment, the $1s$-like core orbitals of the beryllium and fluorine atoms were excluded from the active space. The calculations were performed using the MOLPRO-2002 package of *ab initio* programs.[62]

As has been found at the lower levels of theory,[53–56] the BeF_2 molecule is predicted by the CCSD(T) method to be linear at equilibrium. The calculated equilibrium BeF bond length and total energy are listed in Table I. Both molecular parameters tend to converge to the well-defined asymptotic limits with enlargement of the one-particle basis set. Because BeF_2 is strongly polarized as $F^-Be^{2+}F^-$, we investigated the effects of diffuse functions for fluorine by performing additional calculations with the augmented correlation-consistent basis sets (aug-cc-pVnZ).[63] The calculated equilibrium BeF bond length and total energy are also listed in Table I. Inclusion of the diffuse functions does not affect significantly the molecular parameters. For the basis set of quintuple-zeta quality, the changes are negligibly small, amounting to just 0.0005 Å for the BeF bond length and 2.7 mhartree for the total energy. The effects of core-electron correlation on the molecular parameters were investigated by comparing the values determined in the calculations correlating only the valence electrons (V) with those when all of the electrons were correlated (A), both calculations performed with the correlation-consistent core-valence basis set of quadruple-zeta quality (cc-pCVQZ).[64,65] The difference A-V in the equilibrium BeF bond length was found to be −0.0049 Å. The best estimate of the equilibrium BeF bond length can be determined by adding this difference to the value obtained with the valence basis set of quintuple-zeta quality, thus yielding r_e(BeF)=1.374 Å.

To determine the shape of the potential-energy surface of BeF_2, the total energies were calculated at the CCSD(T)/cc-pV5Z level at 157 points in the vicinity of the equilibrium configuration. The potential-energy surface was then approximated by a three-dimensional expansion along the internal valence coordinates. The internal coordinates for the

TABLE II. The anharmonic force field (the expansion coefficients c_{ijk} of Eq. (1), in hartrees. The coordinates q_1 and q_2 are dimensionless and θ is in radians)

i	j	k	V^a	$V+C^b$
0	0	2	0.026 904	0.027 003
2	0	0	1.228 484	1.235 113
0	0	4	0.004 391	0.004 458
1	1	0	0.123 779	0.128 282
1	0	2	−0.012 949	−0.012 979
3	0	0	−0.788 730	−0.793 361
0	0	6	0.000 009	0.000 024
1	2	0	0.008 771	0.005 412
1	0	4	−0.009 334	−0.009 572
2	0	2	−0.013 999	−0.014 212
1	1	2	0.037 528	0.038 083
4	0	0	−0.139 598	−0.146 752
0	0	8	0.000 467	0.000 469
1	3	0	−0.015 659	−0.018 101
1	0	6	−0.002 312	−0.002 338
3	0	2	−0.005 661	−0.005 901
2	2	0	0.061 191	0.064 818
2	0	4	003 093	0.003 180
1	1	4	0.044 170	0.044 756
1	2	2	−0.032 327	−0.032 255
5	0	0	0.196 252	0.202 194
0	0	10	0.000 025	0.000 024

[a]Determined at CCSD(T)/cc-pV5Z level of theory.
[b]Including additional corrections for the core-electron correlation effects determined at the CCSD(T)/cc-pCVQZ level.

BeF stretching modes q_1 and q_2 were chosen as the Simons-Parr-Finlan coordinates.[66] The FBeF bending mode coordinate θ was defined as the supplement of the valence FBeF angle. The potential-energy surface of BeF$_2$ can be written as the polynomial expansion,

$$V(q_1, q_2, \theta) = V_{\text{lin}} + \sum_{ijk} c_{ijk} q_1^i q_2^j \theta^k, \tag{1}$$

where V_{lin} is the total energy at the linear reference configuration, and the index k takes only even values. The expansion coefficients c_{ijk} were determined from a least-squares fit of Eq. (1) to the computed total energies, and 22 coefficients appeared to be statistically significant. The optimized values of the expansion coefficients are listed in Table II under the column headed "V." Only the coefficients which are not equivalent by symmetry are quoted. To investigate the effects of core-electron correlation on the shape of the calculated potential-energy surface, additional calculations were performed at the CCSD(T)/cc-pCVQZ level. The total energy of BeF$_2$ was computed at the same points as calculated previously, correlating either only valence or all of the electrons. At each point, a difference between these total energies was calculated and added to the valence-only total energy computed at the CCSD(T)/cc-pV5Z level. The calculated potential-energy surface, corrected in this way for the core-related effects, was also approximated by the polynomial expansion of Eq. (1). The optimized values of the expansion coefficients c_{ijk} are listed in Table II under the column headed "$V+C$."

TABLE III. Predicted fundamental vibrational frequencies of BeF$_2$.

	V^a	$V+C^a$
ν_1	764.6	769.7
ν_2	341.0	342.4
ν_3	1549.4	1557.8

[a]Determined using the corresponding anharmonic force field of Table II.

Both potential-energy surfaces were used to calculate the vibration-rotation energy levels of BeF$_2$. The energy levels were calculated variationally using the six-dimensional Hamiltonian for a triatomic molecule by employing the RVIB3 program.[67–69] The Hamiltonian consists of the exact kinetic-energy operator and the potential-energy operator, both expressed in terms of the internal valence coordinates. The symmetry-adapted stretching coordinates (symmetric and antisymmetric) were used. The vibration-rotation energy levels of BeF$_2$, ranging up to about 5000 cm^{-1} above the ground vibrational state, were determined for the rotational quantum number $J=0–8$.[70] The fundamental vibrational frequencies predicted for the two potential-energy surfaces mentioned above are given in Table III. Inclusion of the core-electron correlation affects quite significantly the calculated BeF stretching fundamentals, increasing the ν_1 and ν_3 wave numbers by 5.1 and 8.4 cm^{-1}, respectively. The effective rotational constant for the ground vibrational state B_0 is predicted to be 0.233 10 and 0.234 77 cm^{-1} using the anharmonic force field V and $V+C$, respectively. As we will show below, the spectroscopic constants obtained with the force field $V+C$ are in better agreement with the experimental data than those obtained with the force field V.

III. EXPERIMENT

The experimental details can be found in our previous paper.[1] Gas-phase BeF$_2$ was produced by heating solid BeF$_2$ to about 1000 °C. The emission spectrum was recorded at a resolution of 0.0055 cm^{-1} in the 500–2900-cm^{-1} region with the National Solar Observatory Fourier transform spectrometer at Kitt Peak.

IV. RESULTS AND DISCUSSION

At a temperature of 1000 °C, the $\nu_1+\nu_3$ and $2\nu_2+\nu_3$ combination bands are roughly ten times weaker, and the $\nu_1+\nu_2$ combination band is about 40 times weaker than the ν_3 fundamental band. Figure 1 shows an overview spectrum in the region of the $\nu_1+\nu_3$ combination band. The $10^01(\Sigma_u)–00^00(\Sigma_g)$ band was the strongest combination band and an expanded view is shown in Fig. 2. Nuclear-spin statistics due to the equivalent fluorine nuclei ($I=1/2$) produces a 3:1 intensity alternation. The program WSPECTRA written by Carleer (Université Libre de Bruxelles) was used to determine the line positions. The temperature is sufficiently high that the spectrum contains strong impurity CO emission lines, which were used to calibrate the spectrum. Note that this calibration is an improvement over our previous calibration based on water absorption lines.[1] The absolute accuracy of the measured wave numbers is approximately 0.001 cm^{-1} for the strong bands and 0.002 cm^{-1} for
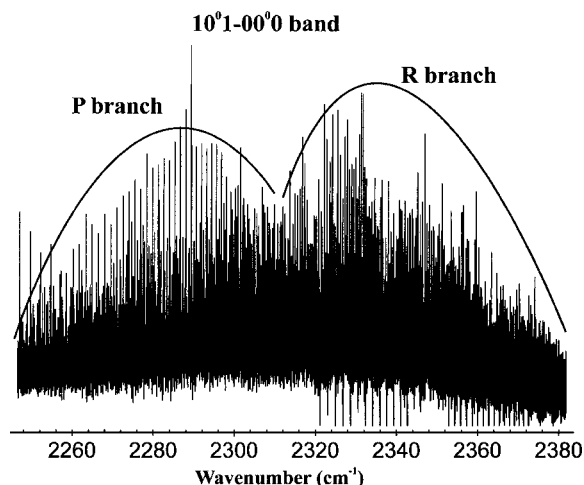
FIG. 1. An overview of the infrared emission spectrum of BeF_2 in the region of the $\nu_1 + \nu_3$ combination band. This spectrum was recorded at the temperature of 1000 °C and the $10^0 1(\Sigma_u) - 00^0 0(\Sigma_g)$ band is the strongest transition in this region.

FIG. 3. An energy level diagram indicating the assigned emission bands for BeF_2. The $11^1 0(\Pi_u) - 00^0 0(\Sigma_g)$ combination band connects all the Π-Π and Σ-Σ transitions together.

the weak transitions. A color LOOMIS-WOOD program was used to pick out the bands.

Figure 3 shows an energy-level diagram indicating the assigned transitions. In the initial stage of our assignments, a least-squares fit was performed for each band that was picked out. The customary energy-level expression for linear triatomic molecules was used,

$$E(J) = G(v_1, v_2^l, v_3) + BJ(J+1) - DJ^2(J+1)^2$$
$$\pm \tfrac{1}{2}[qJ(J+1) + q_D J^2(J+1)^2], \qquad (2)$$

where l is the vibrational angular momentum quantum number ($l = 0, 1, 2,$ and 3 for Σ, Π, Δ, and Φ states, respectively); q and q_D are the l-type doubling parameters, $q = q_D = 0$ for Σ and Φ states, q and q_D are nonzero for Π states, $q = 0$ and $q_D \neq 0$ for Δ states; and the upper (lower) sign refers to the $e(f)$ parity. In Eq. (2), $G(v_1, v_2^l, v_3)$ is the vibrational ($J = 0$) energy of the (v_1, v_2^l, v_3) state relative to the zero-point energy (ZPE), $G(0, 0^0, 0)$. The calculated rotational constants B and D from the variational approach, using the force field $V + C$, agree very well with those obtained from our previous
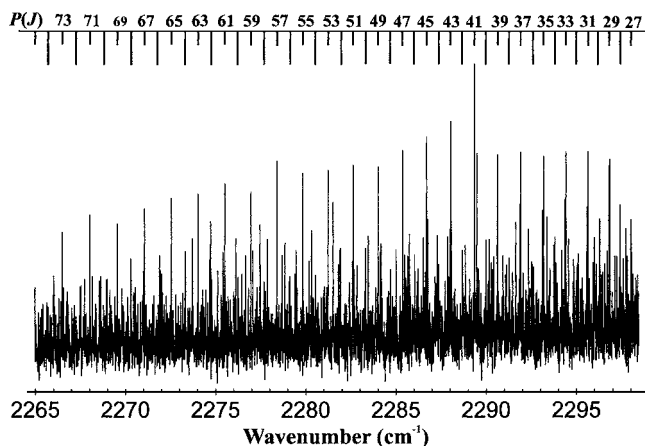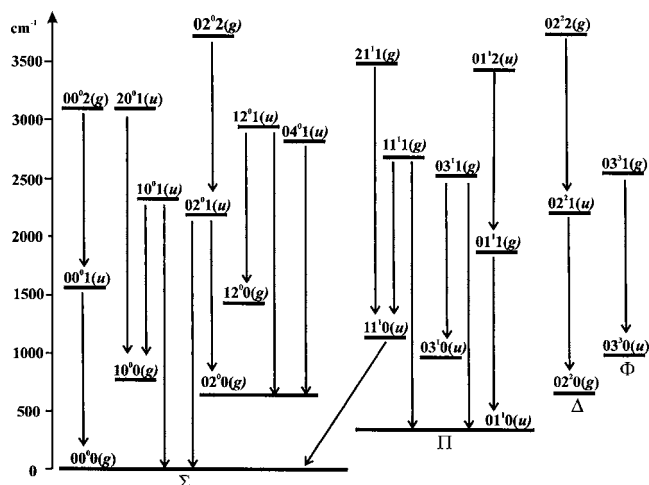

FIG. 2. An expanded view of the P branch of the $10^0 1(\Sigma_u) - 00^0 0(\Sigma_g)$ transition for BeF_2. The 3:1 intensity alternation is due to fluorine nuclear-spin statistics.

study.[1] The predicted rotational constants B and D from the variational approach were thus used to guide our assignments of the new bands. The absolute J assignments of the new $\Sigma - \Sigma$ and $\Pi - \Pi$ bands were obtained by shifting the J assignments until the obtained rotational constants B and D matched the predicted values. The assignments of the combination bands, $11^1 1(\Pi_g) - 01^1 0(\Pi_u)$, $03^1 1(\Pi_g) - 01^1 0(\Pi_u)$, and $21^1 1(\Pi_g) - 11^1 0(\Pi_u)$, were the most difficult. Each of these $\Pi - \Pi$ transitions has four branches, R_e, P_e, R_f, and P_f, but the lines were weak and the spectrum was very congested.

The $11^1 0(\Pi_u) - 00^0 0(\Sigma_g)$ transition connects all of the $\Sigma - \Sigma$ and $\Pi - \Pi$ transitions together (Fig. 3). In the region of the $\nu_1 + \nu_2$ combination band, some fragmentary branches were picked out from the spectrum, but we could not fit any of these branches together to obtain a band. A different method was therefore used to assign this band. Because the spectroscopic constants were available for the upper and lower vibrational levels from other bands, only the band origin of the $11^1 0(\Pi_u) - 00^0 0(\Sigma_g)$ transition was needed to predict the line positions. A value of 1200 cm^{-1} was used for the band origin to predict the line positions and the differences between the adjacent lines were calculated for each of the three predicted branches, P, Q, and R. The differences between the adjacent lines for the Q branch obtained from the experimental data were matched to the values from the predicted Q branch, and the absolute J assignment was obtained. The band origin obtained from the Q branch, 1138.003 cm^{-1}, was then used to pick out the P and R branches from the spectrum.

Finally all assigned $\Sigma - \Sigma$, $\Pi - \Pi$, and $\Pi - \Sigma$ transitions were fitted together. As no band connects the $\Delta - \Delta$ and $\Phi - \Phi$ transitions with the Σ and Π states (Fig. 3), they were fitted separately. The vibrational energies of the $02^2 0(\Delta_g)$ and $03^3 0(\Phi_u)$ could not determined from our experiment and were set to zero in the separate fits. The spectroscopic constants obtained are given in Table IV. The ν_1, ν_2, and ν_3 frequencies were determined from our experiment to be 769.094 33(21), 342.614 53(34), and 1555.047 95(11) cm^{-1},

TABLE IV. Spectroscopic constants (in cm^{-1}) for BeF$_2$ and the difference between the observed and *ab initio* calculated (variational approach using the force field $V+C$) values.

Level	G_v-ZPE Obs.	G_v-ZPE Obs.-Calc.	B Obs.	B Obs.-Calc.	$D/10^{-7}$ Obs.	$D/10^{-7}$ Obs.-Calc.	$q/10^{-4}$ Obs.	$q/10^{-4}$ Obs.-Calc.	$q_D/10^{-9}$ Obs.	$q_D/10^{-9}$ Obs.-Calc.
00^00	0.0	0.0	0.234 984 53(31)	0.000 21	1.008 76(21)	−0.0053				
00^01	1555.047 95(11)	−2.8	0.232 538 14(31)	0.000 20	1.000 27(20)	−0.0054				
00^02	3092.552 90(17)	−5.7	0.230 119 81(32)	0.000 18	0.991 42(22)	−0.0056				
02^00	645.964 43(23)	−0.1	0.236 547 74(34)	0.000 20	1.275 99(26)	−0.0099				
02^01	2188.304 72(19)	−3.0	0.234 180 88(34)	0.000 19	1.269 45(26)	−0.0081				
02^02	3717.800 00(34)	−1.4	0.231 827 64(37)	0.000 16	1.264 08(32)	−0.0045				
12^00	1428.207 66(56)	−1.2	0.235 702 00(59)	0.000 19	1.149 81(92)	−0.0493				
12^01	2960.069 63(46)	−4.2	0.233 326 12(50)	0.000 18	1.160 47(72)	−0.0470				
04^01	2799.097 36(53)	−3.5	0.235 976 27(50)	0.000 19	1.455 26(60)	−0.0348				
10^00	769.094 33(21)	−0.6	0.235 138 71(34)	0.000 22	0.836 31(29)	−0.0196				
10^01	2312.365 87(17)	−3.5	0.232 657 73(34)	0.000 20	0.829 93(30)	−0.0210				
20^01	3089.069 39(36)	−3.8	0.233 473 13(42)	0.000 21	0.674 61(45)	−0.0052				
01^10	342.614 53(34)	0.2	0.236 238 85(31)	0.000 21	1.055 99(19)	−0.0077	−3.8732(20)	0.0095	0.903(28)	−0.56
01^11	1890.444 44(35)	−2.6	0.233 810 85(31)	0.000 20	1.048 44(19)	−0.0081	−3.8013(20)	0.0100	0.969(28)	−0.60
01^12	3420.847 93(55)	−5.6	0.231 407 46(95)	0.000 18	1.007 7(38)	−0.0400	−3.7269(30)	0.0147	⋯	⋯
03^10	969.544 50(45)	−0.2	0.237 703 72(35)	0.000 21	1.267 42(26)	−0.0130	−6.4366(28)	0.0059	5.533(38)	−0.44
03^11	2505.047 52(41)	−3.1	0.235 342 37(34)	0.000 20	1.262 94(26)	−0.0119	−6.3709(26)	0.0042	5.601(38)	−0.47
11^10	1138.003 98(22)	−0.5	0.236 426 46(33)	0.000 22	0.932 07(27)	−0.0133	−5.3166(17)	−0.0072	−2.261(37)	−0.53
11^11	2673.785 63(29)	−3.5	0.233 976 40(32)	0.000 20	0.923 15(23)	−0.0143	−5.1351(19)	−0.0012	−2.084(34)	−0.65
21^11	3472.658 28(31)	−4.4	0.234 539 44(38)	0.000 20	0.816 20(44)	−0.0080	−7.0698(31)	−0.0246	−4.510(66)	−0.17
02^20^a	c	⋯	0.237 489 2(11)	0.000 22	1.097 50(54)	−0.0058	⋯	⋯	−2.868(50)	−0.83
02^21	c+1540.636 44(13)	−2.9	0.235 079 4(11)	0.000 20	1.088 90(53)	0.0006	⋯	⋯	−2.770(50)	−0.67
02^22	c+3063.956 27(31)	−6.0	0.232 698 6(11)	0.000 19	1.094 76(80)	0.0048	⋯	⋯	⋯	⋯
03^30^b	d	⋯	0.238 728 4(11)	0.000 22	1.153 08(62)	−0.0021	⋯	⋯	⋯	⋯
03^31	d+1533.465 39(14)	−3.0	0.236 338 5(11)	0.000 21	1.146 00(63)	0.0008	⋯	⋯	⋯	⋯

[a]The 02^21-02^20 and 02^22-02^21 bands were fitted separately from the other bands, and the value of c was not determined from our experiment and was fixed at 0.0. The value for c obtained from the variational calculation was 686.4 cm^{-1}.
[b]The 03^31-03^30 band was fitted separately from the other bands, and the value of d was not determined from our experiment and was fixed at 0.0. The value for d obtained from the variational calculation was 1031.9 cm^{-1}.

respectively. The observed constants are in very good agreement with the results of our variational calculation, using the force field $V+C$, and the difference is given in Table IV. The difference is in the order of 0.0002 cm^{-1} for the B rotational constants, and a few cm^{-1} for the vibrational energies. The observed line positions and the output files of the least-squares fits are provided in the supplementary Tables S1–S3, which have been placed in the Electronic Physics Auxiliary Publication Service (EPAPS).[71] The uncertainties of 0.001 and 0.002 cm^{-1} were used for most lines of the strong and weak bands, respectively. An uncertainty of 0.005 cm^{-1} was used for blended lines near band origins and band heads.

The 22 vibrational bands were assigned and 20 vibrational levels are connected with each other and with the ground state (Fig. 3). These 20 levels allowed us to derive the equilibrium constants ω_i, x_{ij}, B_e, and α_i for BeF$_2$. The strong Fermi resonance between the $2\nu_2$ and ν_1 vibrational levels exists in the spectrum of BeF$_2$,[1] and the analysis must take this effect into account to obtain accurate constants. The same nonlinear least-squares fitting procedure as used by Cheng et al.[72] and Blanquet et al.[73] to treat CS$_2$ was used. This procedure is based on a method introduced by Pliva.[74] The vibrational ($J=0$) term values and B rotational constants were fitted with the effective Hamiltonians. The effective Hamiltonians take the Fermi resonance into account to give the deperturbed equilibrium constants.

Without Fermi resonance, the vibrational term values are given by the expression

$$G(v_1,v_2^l,v_3) = \sum_i \omega_i\left(v_i + \tfrac{1}{2}d_i\right)$$
$$+ \sum_{i \leq j} x_{ij}\left(v_i + \tfrac{1}{2}d_i\right)\left(v_j + \tfrac{1}{2}d_j\right) + g_{22}l^2, \quad (3)$$

in which d_i is the degeneracy of the ith vibrational mode. These term values form the diagonal elements of the vibrational Hamiltonian matrix. The Fermi resonance shifts both the vibrational and rotational levels and therefore adds the off-diagonal terms which depend on the vibrational and rotational quantum numbers. The off-diagonal terms added to the vibrational ($J=0$) Hamiltonian matrix are[72–74]

$$W_{122} = \langle v_1,v_2,l,v_3,J=0|\hat{H}|v_1-1,v_2+2,l,v_3,J=0 \rangle$$
$$= \frac{1}{2}\{v_1[(v_2+2)^2 - l^2]\}^{1/2}$$
$$\times \left\{ \frac{-k_{122}}{\sqrt{2}} + \lambda_1 v_1 + \lambda_2(v_2+2) \right.$$
$$\left. + \lambda_3\left(v_3 + \frac{1}{2}\right) - \delta l^2 \right\}, \quad (4)$$

where the λ's are the higher-order vibrational corrections and

the constant δ is a vibration-rotation correction. The diagonalization of the vibrational Hamiltonian gives the vibrational energies. The extent of mixing of the vibrational levels is given by the eigenvectors of the vibrational matrix.

The Fermi resonance also changes the B rotational constants. The perturbed B_k values are given in terms of the deperturbed equilibrium constants as[72–74]

$$B_k = \sum_{i,j} V_{ik} V_{jk} F_{ij}, \tag{5}$$

where

$$F_{ii} = B_i^0 = B_e - \alpha_1\left(v_1 + \tfrac{1}{2}\right) - \alpha_2(v_2 + 1) - \alpha_3\left(v_3 + \tfrac{1}{2}\right), \tag{6}$$

$$F_{ij} = \tfrac{1}{2}\delta(v_1)^{1/2}\left[(v_2 + 2)^2 - l^2\right]^{1/2}, \tag{7}$$

and V_{ik} are the eigenvector components from the diagonalization of the vibrational Hamiltonian, with the assumption that the rotational effects are assumed to be too small (i.e., δ is a small correction) to change the eigenvector matrix, **V**. Therefore the observed B rotational constants can be fitted simultaneously with the vibrational ($J=0$) energy levels to give the equilibrium vibrational and rotational constants in Eqs. (3), (4), (6), and (7). This procedure avoids having to work with the complete set of vibration-rotation energy levels and diagonalizing a very large matrix. To save calculation time, the derivatives of the energy eigenvalues with respect to the parameters were computed using the Hellman-Feynman theorem.

Not all the parameters of Eqs. (3), (4), (6), and (7) are independent and a redundancy relationship between x_{22} and x_{ll} ($x_{ll} = g_{22} + B_0$ was fitted instead of g_{22} in the program) has been given by Amat and Pimbert[75] as

$$x_{22} + 3x_{ll} + \frac{(k_{122})^2}{2}\left[\frac{1}{\omega_1} - \frac{1}{2(2\omega_2 + \omega_1)}\right] = 0. \tag{8}$$

The dependence of the parameters can be removed by using the redundancy relation, Eq. (8). The redundancy condition is treated as a data point whose expected value is zero and fitted simultaneously with the observed vibrational energy levels and B rotational constants.

Since the least-squares fit is nonlinear, the initial values of the parameters have to be close to their true values. The Fermi resonance in BeF_2 is very strong and it is not possible to obtain these initial values by hand calculation. A second-order perturbation theory calculation[76,77] was performed to obtain these initial values. The anharmonic force field $V+C$, discussed in Sec. II above, was transformed to curvilinear displacement coordinates and the force constants were calculated from the expansion coefficients c_{ijk} and the equilibrium BeF bond length. As is customary in the perturbation treatment, the anharmonic force field in the displacement coordinates was truncated at quartic order. Because a Fermi resonance of the type $2\omega_2 \approx \omega_1$ occurs, the corresponding anharmonic terms (with near-zero denominators) were removed from the perturbation formulas and the resonance interactions were treated explicitly by diagonalizing an appropriate energy-level matrix. The spectroscopic constants

TABLE V. Spectroscopic constants (in cm^{-1}) for BeF_2.

Constant	Perturbation calculation[a]	Experiment	Variational calculation
ω_1	732.34	731.853(52)	733.77(30)
ω_2	341.00	342.075(19)	341.273(11)
ω_3	1587.87	1584.716(24)	1587.16(14)
x_{11}	−1.331	−1.636(16)	−2.032(96)
x_{12}	−6.155	−5.328(75)	−6.34(32)
x_{22}	1.309	3.149(21)	3.534(91)
x_{13}	−10.197	−10.079(13)	−9.936(78)
x_{23}	−7.336	−7.1708(54)	−7.116(32)
x_{33}	−8.990	−8.7408(67)	−8.641(40)
g_{22}	−2.838	−2.660(19)[b]	−2.814(37)[c]
k_{122}	91.15	90.202(44)	91.23(19)
λ_1	⋯	0.986(17)	1.32(10)
λ_2	⋯	1.093(11)	1.187(54)
λ_3	⋯	−0.0531(59)	−0.110(33)
B_e	0.235 105	0.235 354(41)	0.235 142(25)
α_1	0.000 728	0.000 803(25)	0.000 781(15)
α_2	−0.001 289	−0.001 247(11)	−0.001 238 11(67)
α_3	0.002 480	0.002 424(16)	0.002 410 7(96)
δ	⋯	0.000 4337(84)	0.000 459 9(50)
$\nu_1(\sigma_g)$	766.1	769.094 33(21)	769.7
$\nu_2(\pi_u)$	335.3	342.615 43(34)	342.4
$\nu_3(\sigma_u)$	1557.5	1555.047 95(11)	1557.8
r_e	1.374	1.372 98(12)	1.374

[a]The Fermi resonance constants λ_1, λ_2, λ_3, and δ were not calculated in the perturbation approach.
[b]Calculated from $g_{22} = x_{ll} - B_0$ [$x_{ll} = -2.425(19)$ cm^{-1} from the fit].
[c]Calculated from $g_{22} = x_{ll} - B_0$ [$x_{ll} = -2.579(37)$ cm^{-1} from the fit].

predicted in this way are given in Table V, and the Fermi resonance corrections λ_1, λ_2, λ_3, and δ were not calculated in this calculation.

The equilibrium constants obtained from the experiment are given in Table V and the output file of our fit is given in the supplementary Table S4.[71] Note that the $02^02(\Sigma_g)$ state could not be fitted together with the other states and it was not included. The predicted term value of 3713.1 cm^{-1} for the $02^02(\Sigma_g)$ level is about 5 cm^{-1} smaller than the observed value, 3717.800 00(34) cm^{-1}. One possible reason for this discrepancy is that the $02^02(\Sigma_g)$ state is perturbed by the nearby $42^00(\Sigma_g)$ or/and $50^00(\Sigma_g)$ or/and other states, which were not considered in our fit.

The vibrational ($J=0$) energy levels and B rotational constants from the variational calculation for the same levels as observed in the experiment were also fitted with the same procedure (Table V). The results from the experiment and the calculations agree reasonably well with each other. The experimental value of the Fermi resonance constant k_{122}, 90.202 cm^{-1}, is close to the value of ~80 cm^{-1} for the isoelectronic molecule CO_2,[78] and larger than the value of ~40 cm^{-1} for CS_2.[72]

The constant g_{22} is −2.660 cm^{-1}, which means that for the vibrational states with the same vibrational quantum numbers, as the vibrational angular momentum quantum number l increases, the states go to lower energy if the Fermi resonance is neglected. However, the $02^00(\Sigma_g)$, $02^01(\Sigma_u)$, $02^02(\Sigma_g)$, $03^10(\Pi_u)$, and $03^11(\Pi_g)$ states are pushed down by the Fermi resonance, and finally the $02^20(\Delta_g)$, $02^21(\Delta_u)$, and

$02^22(\Delta_g)$ states lie about 40 cm^{-1} higher than the $02^00(\Sigma_g)$, $02^01(\Sigma_u)$, and $02^02(\Sigma_g)$ states, respectively, and the $03^30(\Phi_u)$ and $03^31(\Phi_g)$ states lie about 60 cm^{-1} higher than the $03^10(\Pi_u)$ and $03^11(\Pi_g)$ states, respectively [from the variational calculations (Table IV)].

The equilibrium rotational constant (B_e) from this fit was used to determine the equilibrium beryllium fluorine distance (r_e) from the moment of inertia equation, and a value of 1.372 98(12) Å (Table V) was obtained. The *ab initio* value is predicted in this study to be 1.374 Å, and it is in remarkably good agreement with the experimental value.

Our new analysis of BeF$_2$ spectra have confirmed our previous tentative assignment of the $\nu_1 + \nu_2$ combination band.[1] The experimental values of ν_1 and ω_1 obtained from the present study are 769.094 33(21), and 731.853(52) cm^{-1}, respectively (Tables IV and V), and ν_1 was estimated to lie between 780 and 890 cm^{-1} in our previous paper.[1] (Remember that ν_1 is the observed fundamental vibrational frequency while ω_1 is the estimated harmonic frequency with the effects of Fermi resonance removed.) However, this assignment was disputed by Lee and Wright[56] based on their harmonic calculations which obtained $\omega_1 = 720 \pm 10$ cm^{-1}, in good agreement with our experimental value of 731.853(52) cm^{-1}. However, their calculations neglected the strong Fermi resonance between the ν_1 and $2\nu_2$ vibrational levels which shifts the ν_1 vibrational frequency by about 40 cm^{-1}. So their conclusion about the value of ν_1 and assignment of the $\nu_1 + \nu_2$ band were incorrect.

V. CONCLUSION

The high-resolution infrared emission spectrum of hot BeF$_2$ was analyzed with the assistance of large-scale *ab initio* calculations. The ν_1, ν_2, and ν_3 vibrational frequencies were determined to be 769.094 33(21), 342.614 53(34), and 1555.047 95(11) cm^{-1}, respectively, from the experimental band origins of the ν_3, $\nu_1 + \nu_3$, and $\nu_1 + \nu_2$ bands. The observed vibrational term values and B rotational constants were fitted simultaneously to an effective Hamiltonian model to obtain equilibrium vibrational and rotational constants ω_i, x_{ij}, B_e, and α_i for the ground electronic state of BeF$_2$ and the Fermi resonance constant k_{122} was found to be 90.202(44) cm^{-1}.

The predicted values for ν_1 obtained from a simple valence force constants analysis[15] (680 cm^{-1}) or from electron diffraction[52] (594 cm^{-1}) are not very reliable, but a modern variational calculation using a high-quality *ab initio* potential-energy surface gives a value (769.7 cm^{-1}) within 0.6 cm^{-1} of the observed one. The agreement between our observed and calculated rotational and centrifugal distortion constants is even more striking. If a small constant offset is removed, then the predictions from the variational calculation essentially match the experimental values within the error bars.

[1] C. I. Frum, R. Engleman, Jr., and P. F. Bernath, J. Chem. Phys. **95**, 1435 (1991).
[2] M. Hargittai, Chem. Rev. (Washington, D.C.) **100**, 2233 (2000).
[3] I. R. Beattie, Angew. Chem., Int. Ed. **38**, 3294 (1999).
[4] V. P. Spiridonov, N. Vogt, and J. Vogt, Struct. Chem. **12**, 349 (2001).
[5] S. H. Ashworth, P. J. Hodges, and J. M. Brown, Phys. Chem. Chem. Phys. **4**, 5923 (2002).
[6] S. H. Ashworth and J. M. Brown, J. Mol. Spectrosc. **191**, 276 (1998).
[7] G. van den Hoek and J. M. Brown, J. Mol. Spectrosc. **182**, 163 (1997).
[8] E. Bosch, P. Crozet, A. J. Ross, and J. M. Brown, J. Mol. Spectrosc. **202**, 253 (2000).
[9] P. A. Akishin and V. P. Spiridonov, Kristallografiya **2**, 475 (1957).
[10] P. A. Akishin, V. P. Spiridonov, and G. A. Sobolev, Dokl. Akad. Nauk SSSR **118**, 1134 (1958).
[11] L. Wharton, R. A. Berg, and W. Klemperer, J. Chem. Phys. **39**, 2023 (1963).
[12] A. Büchler, J. L. Stauffer, and W. Klemperer, J. Am. Chem. Soc. **86**, 4544 (1964).
[13] A. Büchler, J. L. Stauffer, and W. Klemperer, J. Chem. Phys. **40**, 3471 (1964).
[14] M. Hargittai, Coord. Chem. Rev. **91**, 35 (1988).
[15] A. Snelson, J. Phys. Chem. **70**, 3208 (1966).
[16] D. E. Mann, G. V. Calder, K. S. Seshadri, D. White, and M. J. Linevsky, J. Chem. Phys. **46**, 1138 (1967).
[17] V. Calder, D. E. Mann, K. S. Seshadri, M. Linevsky, and D. White, J. Chem. Phys. **51**, 2093 (1969).
[18] D. White, G. V. Calder, S. Hemple, and D. E. Mann, J. Chem. Phys. **59**, 6645 (1973).
[19] R. H. Hague, J. L. Margrave, and A. S. Kana'an, J. Chem. Soc., Faraday Trans. 2 **71**, 1082 (1975).
[20] M. L. Lesiecki and J. W. Nibler, J. Chem. Phys. **64**, 871 (1976).
[21] F. Ramondo, V. Rossi, and L. Bencivenni, Mol. Phys. **64**, 513 (1988).
[22] E. F. Hayes, J. Phys. Chem. **70**, 3740 (1966).
[23] J. L. Gole, A. K. Q. Siu, and E. F. Hayes, J. Chem. Phys. **58**, 857 (1973).
[24] C. A. Coulson, Isr. J. Chem. **11**, 683 (1973).
[25] N. M. Kilmenko, D. G. Musaev, and O. P. Charkin, Russ. J. Inorg. Chem. **29**, 639 (1984).
[26] U. Salzner and P. von R. Schleyer, Chem. Phys. Lett. **172**, 461 (1990).
[27] D. M. Hassett and C. J. Marsden, Chem. Commun. (Cambridge) **1990**, 667 (1990).
[28] L. Seijo, Z. Barandiarán, and S. Huzinaga, J. Chem. Phys. **94**, 3762 (1991).
[29] T. G. Wright, E. P. F. Lee, and J. M. Dyke, Mol. Phys. **73**, 941 (1991).
[30] M. Kaupp and P. v. R. Schleyer, J. Am. Chem. Soc. **114**, 491 (1992).
[31] D. M. Hasset and C. J. Marsden, J. Mol. Struct. **346**, 249 (1995).
[32] D. Cubiciotti, J. Phys. Chem. **65**, 1058 (1961).
[33] T. E. Brackett and E. B. Brackett, J. Phys. Chem. **66**, 1542 (1962).
[34] A. Büchler, W. Klemperer, and A. G. Emslie, J. Chem. Phys. **36**, 2499 (1962).
[35] I. Eliezer, Theor. Chim. Acta **18**, 77 (1970).
[36] I. Eliezer and A. Reger, Theor. Chim. Acta **26**, 283 (1972).
[37] Y. S. Kim and R. G. Gordon, J. Chem. Phys. **60**, 4332 (1974).
[38] M. Guido and G. Gigli, J. Chem. Phys. **65**, 1397 (1976).
[39] M. Guido and G. Gigli, J. Chem. Phys. **66**, 3920 (1977).
[40] D. L. Hildenbrand, J. Electrochem. Soc. **126**, 1396 (1979).
[41] M. Spoliti, G. DeMaria, L. D'Alessio, and M. Maltese, J. Mol. Struct. **67**, 159 (1980).
[42] G. Galli and M. P. Tosi, Nuovo Cimento Soc. Ital. Fiz., **4D**, 413 (1984).
[43] W. Andreoni, G. Galli, and M. Tosi, Phys. Rev. Lett. **55**, 1734 (1985).
[44] I. Bytheway, R. J. Gillespie, T.-H. Tang, and R. F. W. Bader, Inorg. Chem. **34**, 2407 (1995).
[45] K. J. Donald, W. H. Mulder, and L. V. Szentpály, J. Chem. Phys. **119**, 5423 (2003).
[46] M. Kaupp, Angew. Chem., Int. Ed. **40**, 3534 (2001).
[47] R. L. De Kock, M. A. Peterson, L. K. Timmer, E. J. Baerends, and P. Vernooijs, Polyhedron **9**, 1919 (1990).

[48] L. von Szentpály and P. Schwerdtfeger, Chem. Phys. Lett. **170**, 555 (1990).

[49] M. Kaupp, P. v. R. Schleyer, H. Stoll, and H. Preuss, J. Am. Chem. Soc. **113**, 6012 (1991).

[50] L. von Szentpály, J. Phys. Chem. A **106**, 11945 (2002).

[51] A. Büchler and W. Klemperer, J. Chem. Phys. **29**, 121 (1958).

[52] N. Vogt, G. V. Girichev, J. Vogt, and A. G. Girichev, J. Mol. Struct. **352/353**, 175 (1995).

[53] J. M. Dyke and G. Wright, Chem. Phys. Lett. **169**, 138 (1990).

[54] F. Ramondo, L. Bencivenni, and M. Spoliti, J. Mol. Struct.: THEOCHEM **277**, 171 (1992).

[55] T. P. Pogrebnaya, V. V. Sliznev, and V. G. Solomonik, Koord. Khim. **23**, 498 (1997).

[56] E. P. F. Lee and T. G. Wright, J. Phys. Chem. A **104**, 974 (2000).

[57] J. Čížek, J. Chem. Phys. **45**, 4256 (1966).

[58] G. D. Purvis III and R. J. Bartlett, J. Chem. Phys. **76**, 1910 (1982).

[59] K. Raghavachari, G. W. Trucks, J. A. Pople, and M. Head-Gordon, Chem. Phys. Lett. **157**, 479 (1989).

[60] G. E. Scuseria and T. J. Lee, J. Chem. Phys. **93**, 5851 (1990).

[61] T. H. Dunning, Jr., J. Chem. Phys. **90**, 1007 (1989).

[62] H.-J. Werner, P. J. Knowles, R. D. Amos *et al.*, MOLPRO-2002, package of *ab initio* programs.

[63] R. A. Kendall, T. H. Dunning, Jr., and R. J. Harrison, J. Chem. Phys. **96**, 6796 (1992).

[64] D. E. Woon and T. H. Dunning, Jr., J. Chem. Phys. **103**, 4572 (1995).

[65] D. E. Woon, K. A. Peterson, and T. H. Dunning, Jr. (unpublished).

[66] G. Simons, R. G. Parr, and J. M. Finlan, J. Chem. Phys. **59**, 3229 (1973).

[67] S. Carter and N. C. Handy, Mol. Phys. **57**, 175 (1986).

[68] S. Carter and N. C. Handy, Comput. Phys. Rep. **5**, 117 (1986).

[69] N. C. Handy, Mol. Phys. **61**, 207 (1987).

[70] An exhaustive list of the calculated vibration-rotation energy levels of BeF_2 can be obtained from us upon request.

[71] See EPAPS Document No. E-JCPSA6-123-007534 for the observed line positions and the output files of the least-squares fits for all the bands (Tables S1–S3), and the output file of the Fermi resonance molecular constant fit (Table S4). This document can be reached via a direct link in the online article's HTML reference section or via the EPAPS homepage (http://www.aip.org/pubservs/epaps.html).

[72] C.-L. C. Cheng, J. L. Hardwick, and T. R. Dyke, J. Mol. Spectrosc. **179**, 205 (1996).

[73] G. Blanquet, E. Baeten, I. Cauuet, J. Walrand, and C. P. Courtoy, J. Mol. Spectrosc. **112**, 55 (1985).

[74] J. Pliva, J. Mol. Spectrosc. **27**, 461 (1968).

[75] G. Amat and M. Pimbert, J. Mol. Spectrosc. **16**, 278 (1965).

[76] D. Papousek and M. R. Aliev, *Molecular Vibrational Rotational Spectra* (Academia, Prague, 1982).

[77] J. F. Gaw, A. Willetts, W. H. Green, and N. C. Handy, in *Advances in Molecular Vibrations and Collision Dynamics*, edited by J. M. Bowman (JAI, Greenwich, CT, 1990).

[78] S. A. Tashkun, V. I. Perevalov, J.-L. Teffo, L. S. Rothman, and V. G. Tyuterev, J. Quant. Spectrosc. Radiat. Transf. **60**, 785 (1998).